Submitted to
Journal of Physics D: Applied Physics

Supersonic metal plasma impact on a surface:

An optical investigation of the pre-surface region

Pavel A. Ni and André Anders*
Lawrence Berkeley National Laboratory, University of California, 1 Cyclotron Road, Berkeley, California 94720, USA

December 15, 2009

ACKNOWLEDGMENT
The work was supported by the US Department of Energy under Contract No DE-AC02-05CH11231 with the Lawrence Berkeley National Laboratory.

* Author to whom correspondence should be addressed. Electronic mail: aanders@lbl.gov

Supersonic metal plasma impact on a surface:

An optical investigation of the pre-surface region

Pavel A. Ni and André Anders*

Lawrence Berkeley National Laboratory, University of California, 1 Cyclotron Road, Berkeley, California 94720, USA

Abstract

Aluminum plasma, produced in high vacuum by a pulsed, filtered cathodic arc plasma source, was directed onto a wall where if formed a coating. The accompanying "optical flare" known from the literature was visually observed, photographed, and spectroscopically investigated with appropriately high temporal (1 μs) and spatial (100 μm) resolution. Consistent with other observations using different techniques, it was found that the impact of the fully ionized plasma produces metal neutrals as well as desorbed gases, both of which interact with the incoming plasma. Most effectively are charge exchange collisions between doubly charged aluminum and neutral aluminum, which lead to a reduction of the flow of doubly charged before they reach the wall, and a reduction of neutrals as the move away from the surface. Those plasma-wall interactions are relevant for coating processes as well as for interpreting the plasma properties such as ion charge state distributions.

1. Introduction

The interaction of condensable (metal) plasma with surfaces is generally not widely investigated – it appears as a topic of mostly academic interest. However, plasma-wall interaction of this type occurs in all systems where such plasma is created, be it by pulsed laser ablation [1-2], cathodic arcs [3-4], high power impulse magnetron sputtering [5], or via ion acceleration in the sheath of biased systems, like with plasma immersion processing [6]. In fact, it is very widely used if one includes various kinds of plasma-based and plasma-assisted deposition of hard, wear-resistant, or corrosion-resistant coatings [7-9], and metallization of semiconductor processors, including barrier layer deposition and filling of vias and trenches [6, 10-12]. In this sense, a huge number of components of modern every-day live are affected.

Due to the large variety of possible situations in terms of material combination, energy distributions, etc., the most successful so far are molecular dynamics (MD) computer simulations applied to specific materials and energy ranges of interest [13-15], like the one needed for three-dimensional chip processing or fabrication of micro-electro-mechanical system (MEMS) devices.

Apart from the importance for the coatings and devices, there is a feedback of the plasma-wall interaction on the plasma itself due to the particles that leave the surface and enter the plasma. Among those particles are desorbed gases, sputtered atoms, and reflected ions; the latter are usually neutralized upon interaction with the surface and appear in the

* Author to whom correspondence should be addressed. Electronic mail: aanders@lbl.gov

plasma as energetic neutrals [16]. This means, the vast majority of events lead to neutrals entering the plasma, as opposed to ions, and the neutrals will cause elastic and inelastic electron-neutral and ion-neutral collisions, which change the plasma as apparent by a reduction of the mean ion charge state [17]. The situation is not trivial for condensable (metal) plasmas, and the consequences for the plasma parameters themselves are often not appreciated.

In this contribution, we will use *optical* methods to demonstrate that the surface is indeed a source of particles influencing the plasma even for the case of a plasma with condensable ions. The plasma in the experiment is a fully ionized metal plasma exiting the curved macroparticle filter of a pulsed cathodic arc source, very similar to a companion paper where the emphasis was on film growth as a function of incident angle [18].

A motivating starting point of the investigation was the striking enhancement of optical emission near the surface as shown in Fig. 1. Similar observations were reported before, for example by Tarrant and co-workers [19]. Here, we will describe the plasma and show the appearance of neutrals using optical emission spectrometry and time-resolving streak camera photography. This work supplements previous reports where the effects of neutrals on ion charge states were discussed [17], and where the thickness of coatings on tilted surfaces was used to estimate the magnitude of non-sticking and self-sputtering [18].

2. Experimental details

A supersonic plasma flow can readily be made using a filtered cathodic arc plasma source [20]. 'Supersonic' refers to the fact that the ion streaming velocity exceeds the ion sound velocity, which results in a typical Mach number of 3-5 depending on material and other conditions [21]. Aluminum was selected as the cathode material, and the resulting cathodic arc plasma flow is dominated by doubly charged aluminum ions as previously determined by time-of-flight spectrometry [21-22].

The principal experimental setup is shown in Fig. 2. The plasma source was a cathodic arc of the "minigun type" [20] consisting of a ¼ inch (6.25 mm) diameter cathode placed on axis of an annular, grounded anode body. The cathode material was placed in a ceramic tubing ensuring that the cathode spots can only operate at the front surface of the cathode rod. The cathode material can be selected freely, and here we opted to use Al for its suitable emission lines of ions and atoms in the accessible spectral range (350 nm to 800 nm). The arc discharge was fed by a pulse forming network, giving a near-rectangular current pulse of 800 A with a duration of about 800 µs (full width at half maximum).

The flowing plasma expanded in vacuum after leaving the macroparticle (and neutral atom) filter, until it interacted with the intentionally positioned wall. An enhanced glow can be observed visually, which is also shown in Fig. 1 and schematically indicated in Fig. 2. This light emission was projected with a lens onto optical fibers as indicated in Fig. 2. The fiber position can be accurately adjusted via a precision mount on an optical rail. In this way, spatial resolution in z-direction, the direction normal to the wall's surface, was obtained with 0.1 mm accuracy. Two fibers were used: one couples light into a moderately-high-resolving spectrometer (PCM 420 by Telemark, spectral range 350 nm to 1050 nm, $\Delta\lambda \sim 0.05$ nm), and the other into a less-resolving spectrometer (Horiba Jobin

Yvon CP140, $\Delta\lambda \sim 1\,\mathrm{nm}$) attached to a streak camera (Hamamatsu C7700) equipped with a dual-scan, cooled CCD camera (Hamamatsu C4880) sensitive in the 350-900 nm spectral range [23]. The detector of the higher resolving spectrometer integrates the light over the entire duration of a plasma pulse, whereas the streak camera system allows us to study the evolution of the emission with temporal resolution. In order to cover the total duration pulse of 1 ms with the streak, we used a slowest sweep speed of the streak camera giving us 1 μs resolution, which is more than sufficient for the this study.

3. Results

3.1 Photography

The first results are time integrated photographs such as the one shown in Fig. 1. They were obtained with a conventional digital single lens reflex camera equipped with a CMOS detector chip (Canon EOS 300D), operated in open-shutter "bulk" mode to capture an entire arc pulse event. The figure represents the original image (no filters applied) except that the contrast was slightly enhanced to better show the difference of light intensity at the filter exit and the near-surface zone. Such images are the reason why we expected to derive information using more sophisticated time and space resolving imaging techniques.

3.2 Spatially resolved, time-integrated spectroscopy

A next step was to identify the kind of radiation using the modestly high-resolving spectrometer. Fig. 3 illustrates some results of the spectral analysis for the spectral range from 385 nm 485 nm. One can see that the spectrum contains lines of neutral (Al I), singly ionized (Al II) and doubly ionized (Al III) aluminum as well as molecular bands ("not aluminum") which we associate with desorbed gases. This will allow us to draw qualitative or even semi-quantitative conclusions about the evolution of the ratios of the species which, as mentioned before, was a main reason why aluminum was selected from the many possible cathode materials.

A first-glance comparison of the two spectra reveals that the lines of neutral aluminum, Al I, are much more intense in the immediate vicinity of the surface. One should note that the intensity is plotted on a logarithmic scale covering several orders of magnitude. Besides aluminum, there are some broad bands of emission lines that are not associated with aluminum, rather, the emission seems to be associated with the excitation of desorbed gases which are typical for processing in high vacuum (as opposed to ultrahigh vacuum).

As one can further see in Fig. 3, several spectral lines that are marginally resolved with the PCM 420 are from the *same* ion charge state. This is a fortunate feature of the aluminum spectrum that is later utilized when making the time-resolving measurements with the less spectrally-resolving streak-camera system. Because they are all from the same charge state, the group of merged lines can be used for measurements of the temporal evolution of that charge state. For example, the neutral lines Al I 394.4 nm and 396.15 nm form such group, as well as the lines Al II 364.86 nm, 366.31 nm 366.68 nm of the singly charged ions, and the Al III 447.99 nm, 448.0 nm, 451.25 nm and 352.92 nm lines of the doubly charged ions. We will elaborate on those measurements in the next section dealing with time-resolved data.

3.3 Spatially and temporally resolved spectroscopy

The combination of a spectrometer and a streak camera allowed us to investigate the temporal evolution of the spectra. As in the previous experiment, the spatial resolution was established in one dimension, namely for the z-axis or distance from the surface, by positioning the light-collecting fiber as indicated in Fig. 2. Each set of measurements was repeated several times, with the direction of the z-axis motion reversed in order to minimize the influence of drifts that possibly could be associated with the plasma production (although we did not have any indication for such drifts). As a result, the data obtained were averaged over typically six individual measurements.

Fig. 4 shows an example of time-resolved spectra obtained at two different distances from the surface, namely the immediate vicinity of the surface and 20 mm away from the surface. Most strikingly, one can see dramatic differences in the intensity of neutral lines around 396 nm, which are 10 times stronger on the surface than in 20 mm distance. We note that the intensity of the doubly charged ions fluctuates much stronger than the intensity of the lines of singly charged ions and neutrals, which will be discussed in section 4.

Another presentation of the temporal evolution of the light intensity emitted by various species is shown in Fig. 5. One can see that the lines emitted by neutral aluminum (Al I) and by the desorbed gases seem to appear *before* the ion lines are visible. Lines of Al III decay much faster than the other lines, on a timescale of ~ 0.5 ms, and this effect is more pronounced further away from the surface. Also here, one can see that the intensities of the Al III lines are generally much more fluctuating ("noisy") than the intensities of singly charged or neutral species.

The wealth of time-resolved data can be used to obtain reduced but meaningful information. One can integrate each line (or a group of lines of the same charge state, as mentioned before) over the pulse duration and plot the cumulative intensities as a function of distance from the surface (Fig. 6).

Despite the averaging over six individual measurements, it is evident from Fig. 6 that the intensities of the Al III lines are much noisier than the intensities of the other species, which was already noted when describing Fig. 4. However, more importantly and interestingly, the character of the spatial dependence is very different for the different species, which must be related to the presence of the wall and the plasma-surface interaction.

One can clearly see that intensity of light emitted by neutrals, both of aluminum and desorbed gases, is highest at the surface and decays rapidly within 20 mm distance. The intensity of singly charged aluminum, Al II, stays relatively flat, while the Al III lines are strongest far from the wall. Those features will be discussed in the next section.

4. Discussion

Much is known about the cathodic arc plasma [4, 21, 24-26] but relatively little about the interactions of the plasma with the surface of a solid wall. Generally, the arc plasma can condense on a surface and forms a deposit or film [3], which is widely used, for example for the fabrication of superhard coating of TiAlN on cutting tools [27]. The ion energy and charge states play an important role for the properties coating, in terms of film density, microstructure, stress, etc. In previous publications [17-18, 28], the role of neutrals on the

coating and on the plasma itself was stressed, and the observations presented here should be seen as a further contribution clarifying the formation and influence of neutrals.

Starting with Fig. 1, one can immediately see that the presence of the surface greatly affects the plasma flow. If the ions of the condensable plasma had a sticking coefficient of unity, and desorption and self-sputtering were negligible, no such "optical flare" (as called by Tarrant and co-workers [19]) could be observed. Clearly, a combination of non-sticking, desorption, and self-sputtering must be there to produce particles which interact with the incoming plasma flow. It is known that such processes produce neutral atoms, as opposed to ions. Therefore, visual and photographic observations already provide strong evidence that *a wall impacted by fully ionized metal plasma is a source of neutrals*.

In the present experiment, aluminum was selected as the metal plasma because one can find strong lines of neutrals and ions in the visible part of the spectrum. As Fig. 3 showed, the time-integrated spectra show aluminum neutrals and ions as well as lines and bands that can be attributed the desorbed gases. The bands are not resolved but it is likely that they include the second positive system of N_2 (e.g. 427 nm, 435.5 nm, 441.6 nm), the first negative system of N_2^+ (e.g. 427.8 nm), and bands of CH (e.g. at 431.4 nm) [29].

Figs. 4 and 6, dealing with the time resolved emission data, indicate that the neutral lines appeared *before* the lines of aluminum ions became visible. This initially puzzling feature can be understood recalling that the plasma exciting the macroparticle filter is in thermodynamic non-equilibrium because it expands rapidly. The rate of expansion is fast enough that collisions are insufficient to bring specific parts of the system to equilibrium: in this case we consider free electrons on the one hand and the population of excited electronic levels of ions on the other. One can define a corresponding dimensionless Damköhler number for the excitation rates in relation to the expansion rate and find it less than unity. Non-equilibrium means that the upper electronic levels of ions are underpopulated and hence radiation from those ions is weak, or, simply said: the plasma appears much darker than if it was in equilibrium. As the non-equilibrium flow hits the wall, most metal ions are deposited but some do not stick and but are reflected and neutralized in the process, which is known from computer simulations (e.g. [14][15]) and experiments like those described in the companion paper [18]). Metal atoms and the desorbed gas molecules collide with the plasma ions, slow them, and the free electrons put the ions closer to equilibrium, i.e. they "light up". The fact that we then see intense lines of doubly charged aluminum (Al III spectrum) is reasonable because it is known from the literature that cathodic arc aluminum plasma is dominated by doubly charged ions while the densities of Al^+ (Al II spectrum) and Al^0 (Al I spectrum) are much lower [21-22]

The spatial distribution of line intensities is in agreement with this scenario. As the plasma is approaching the wall, it encounters the opposing flow of neutrals, and charge exchange collisions of the types

$$Al^{Q+} + Al^0 \rightarrow Al^{(Q-1)+} + Al^+ \quad (1)$$

$$Al^{Q+} + G^0 \rightarrow Al^{(Q-1)+} + G^+ \quad (2)$$

can occur, which result in the reduction of the multiply charged ions; here, G stands for a gas atom or molecule, and Q is the charge state number. The process (2) is not effective for

singly charged aluminum, $Q=1$, because the energy defect (potential energy difference before and after the collision) is not positive; details on energy defect are further discussed ref.[17, 30]. As a given volume element of the plasma flow is getting closer to the wall, more and more of its multiply charged ions are recombined, and hence one should expect a deduction of the associated emission from doubly charged ions. Singly charged ions, however, are produced in the charge exchange process, and the observed Al II lines do not fall as the lines of Al III do.

It was noted that the intensity of Al III fluctuates stronger than the intensity of lower charge states. This is consistent with observations based on ion charge state spectrometry [31]. Those fluctuations rooted in the fractal nature of the cathode processes [4].

Interestingly, and consistently, the metal and non-metal neutral lines show the same general features, namely a peak near the surface and decay as the neutrals move away from the wall surface. One of the reasons for the decay is the "consumption" of neutral aluminum atoms by the charge exchange process (1). Indeed, the rate of "decay" of Al I shown in Fig. 6 is greater than the rate of decay of the desorbed gas neutrals.

5. Conclusion

Fully ionized aluminum plasma, produced by pulsed, filtered cathodic arc system, was flowing against a wall, and the region near the wall was spectroscopically investigated with spatial and temporal resolution in order to gain deeper insight of the interaction of the metal plasma with the wall. In agreement with previous studies using other techniques, we found that a significant amount of metal does not stick to the wall but returns to the plasma as neutrals. Both metal neutrals and desorbed gas has been indentified. The flow of neutrals reduces the intensity of doubly charged ions as they approach the surface, and the intensity of line emission from neutrals reduces as they move from the surface. Both features can be explained by charge exchange collisions. The present study is another, independent confirmation of the source of neutrals, i.e. the plasma itself interacting with a wall, and the role of the neutrals play for the plasma composition.

Acknowledgments

The work was supported by the US Department of Energy under Contract No DE-AC02-05CH11231.

References

[1] Chrisey D B and Hubler G K (Ed.) *Pulsed Laser Deposition of Thin Films*. New York: Wiley, 1994.

[2] Franghiadakis Y, Fotakis C, and Tzanetakis P *J. Appl. Phys.* 1998 **84** 1090-1094.

[3] Brown I G *Annual Rev. Mat. Sci.* 1998 **28** 243-269.

[4] Anders A, *Cathodic Arcs: From Fractal Spots to Energetic Condensation*. New York: Springer, 2008.

[5] Ehiasarian A P, Wen J G, and Petrov I *J. Appl. Phys.* 2007 **101** 054301-10.

[6] Monteiro O R *J. Vac. Sci. Technol. B* 1999 **17** 1094-1097.

[7] Monteiro O R *Nucl. Instrum. Meth. Phys. Res. B* 1999 **148** 12-16.

[8] Gorokhovsky V, Heckerman B, Watson P, and Bekesch N *Surf. Coat. Technol.* 2006 **200** 5614-5630.

[9] Wei R (Ed.) *Plasma Surface Engineering Research and its Practical Applications* Singapore: Rsearch Signpost, 2008.

[10] Rossnagel S R and Hopwood J *J. Vac. Sci. Technol. B* 1994 **12** 449-453.

[11] Beilis I I, Grach D, Shashurin A, and Boxman R L *Microelectronic Engineering* 2008 **85** 1713-1716.

[12] Klepper C C, Monteiro O R, Carlson E P, and Keitz M D *J. Vacuum Sci. Technol. B* 2009 **27** L14-L17.

[13] Müller K-H *J. Appl. Phys.* 1987 **62** 1796-1799.

[14] Kress J D, Hanson D E, Voter A F, Liu C L, Liu X Y, and Coronell D G *J. Vac. Sci. Technol. A* 1999 **17** 2819-2825.

[15] Hanson D E, Stephens B C, Saravanan C, and Kress J D *J. Vac. Sci. Technol. A* 2001 **19** 820-825.

[16] Winters H F, Coufal H J, and Eckstein W *J. Vac. Sci. Technol. A* 1993 **11** 657-663.

[17] Anders A, Oks E M, and Yushkov G Y *J. Appl. Phys.* 2007 **102** 043303.

[18] Wu H and Anders A *J. Phys D: Appl. Phys.* 2009 submitted; under review.

[19] Tarrant R N, Bilek M M M, Pigott J, and McKenzie D R *Surf. Coat. Technol.* 2004 **186** 10-16.

[20] MacGill R A, Dickinson M R, Anders A, Monteiro O R, and Brown I G *Rev. Sci. Instrum.* 1998 **69** 801-803.

[21] Anders A and Yushkov G Y *J. Appl. Phys.* 2002 **91** 4824-4832.

[22] Brown I G *Rev. Sci. Instrum.* 1994 **65** 3061-3081.

[23] Ni P A, Bieniosek F M, Leitner M, Weber C, and Waldron W L *Nucl. Instrum. Meth. Phys. Res. A* 2009 **606** 169-171.

[24] Lunev V M, Padalka V G, and Khoroshikh V M *Sov. Phys. Tech. Phys.* 1977 **22** 858-861.

[25] Davis W D and Miller H C *J. Appl. Phys.* 1969 **40** 2212-2221.

[26] Boxman R L, Sanders D M, and Martin P J (Ed.) *Handbook of Vacuum Arc Science and Technology*. Park Ridge, N.J.: Noyes Publications, 1995.

[27] Coll B F, Fontana R, Gates A, and Sathrum P *Mater. Sci. Eng. A* 1991 **140** 816-824.

[28] Anders A *IEEE Trans. Plasma Sci.* 2005 **33** 205-209.

[29] Pearse R W B and Gaydon A G, *Identification of Molecular Spectra*, 4th ed. New York: Wiley, 1976.

[30] Bransden B H and McDowell M R C, *Charge Exchange and the Theory of Ion-Atom Collisions*. Oxford, UK: Clarendon Press, 1992.
[31] Anders A *IEEE Trans. Plasma Sci.* 1999 **27** 1060-1067.

Figure Captions

Fig. 1 (color online) Enhanced optical emission in front of a surface (left) hit by cathodic vacuum arc copper plasma (steaming from the right); open shutter photograph through the vacuum window; the plasma duration was 1 ms – for further details consult section 2 and the remainder of the text.

Fig. 2 (color online) Experimental setup: a pulsed filtered cathodic vacuum arc synchronized with a streak camera; the pre-surface region was imaged on to optical fibers feeding a moderately high resolution spectrometer and a lower resolution spectrometer with a streak camera detector.

Fig. 3 (color online) Optical emission in the spectral range 385 nm to 485 nm of aluminum arc plasma hitting an aluminum wall; the top spectrum shows the emission in the immediate vicinity of the surface, while to lower spectrum is the light emitted in the zone 10 mm from the surface.

Fig. 4 (color online) Time-resolved spectra for two different positions: top: immediate vicinity of the surface; bottom: 20 mm from the surface (contrast was enhanced for better visibility, no camera spectral sensitivity corrections were applied). Note the huge difference in Al I intensity.

Fig. 5 (color online) Evolution of light emission from a region within 1 mm of the surface and 23 mm from the surface (example of a single discharge pulse – no averaging applied). Emission intensities of Al I, Al II, Al III lines as indicated in Fig. 3, and emission from gas in the spectral region 425-430 nm were numerically added to create a representative emission from each of the species as a function of time.

Fig. 6 (color online) Sum of time-integrated intensities of spectral lines of aluminum neutral, singly charged, doubly charged ions, and emission from desorbed gas molecules, plotted as a function of the distance from the surface. Each data point is the average of 6 individual measurements and time integrations.

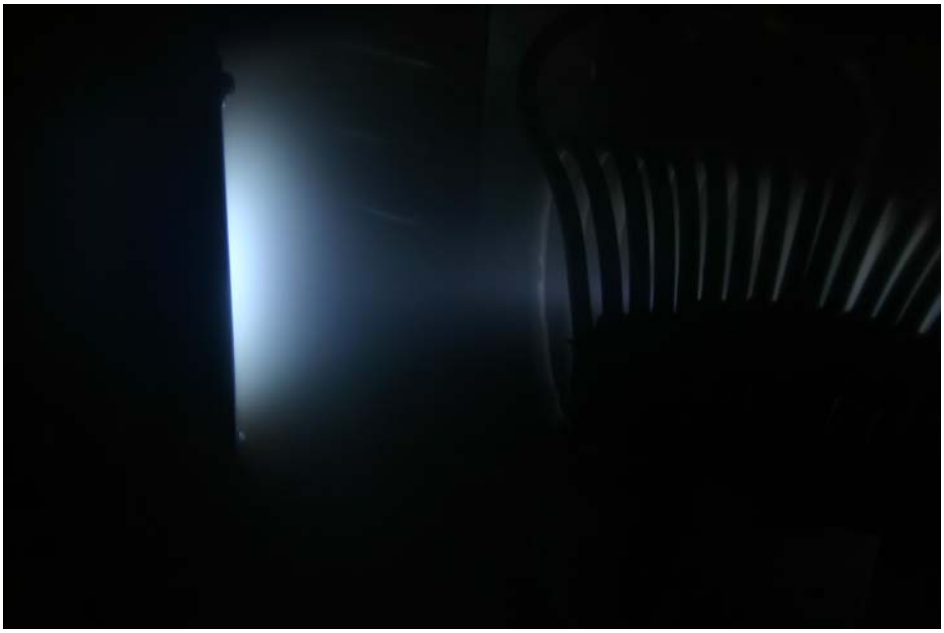

Fig. 1

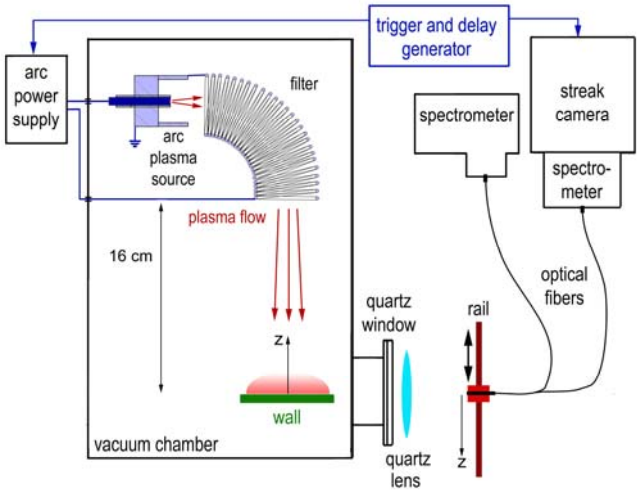
trigger and delay generator
arc power supply
filter
arc plasma source
plasma flow
16 cm
z
wall
vacuum chamber
quartz window
quartz lens
rail
z
spectrometer
streak camera
spectro-meter
optical fibers

Fig. 2

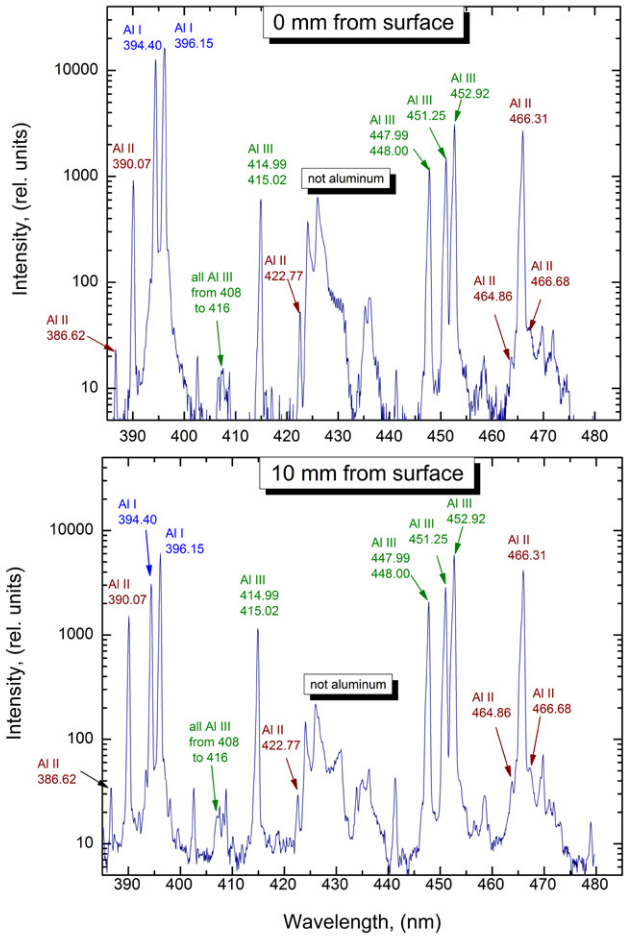
0 mm from surface
Al I 394.40
Al I 396.15
Al II 390.07
Al III 414.99 415.02
not aluminum
Al III 447.99 448.00
Al III 451.25
Al III 452.92
Al II 466.31
all Al III from 408 to 416
Al II 422.77
Al II 464.86
Al II 466.68
Al II 386.62
10 mm from surface
Intensity, (rel. units)
Wavelength, (nm)

Fig. 3

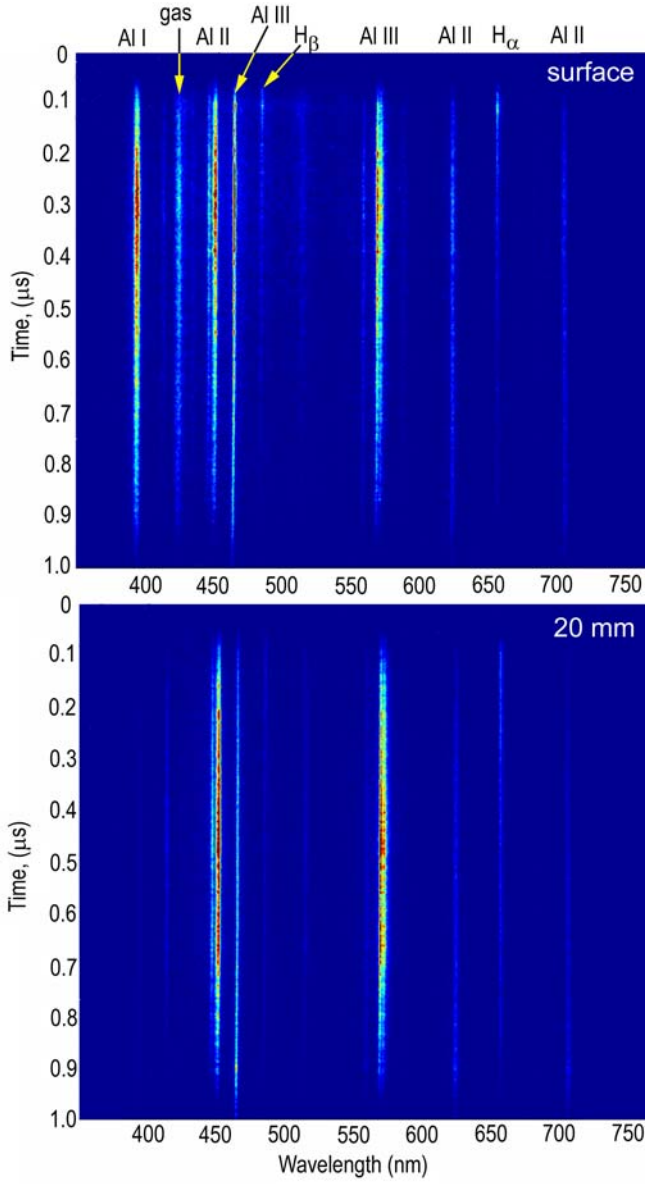
gas
Al I
Al II
Al III
Hβ
Al III
Al II
Hα
Al II
surface
20 mm
Time, (μs)
Wavelength (nm)
0
0.1
0.2
0.3
0.4
0.5
0.6
0.7
0.8
0.9
1.0
400
450
500
550
600
650
700
750

Fig. 4

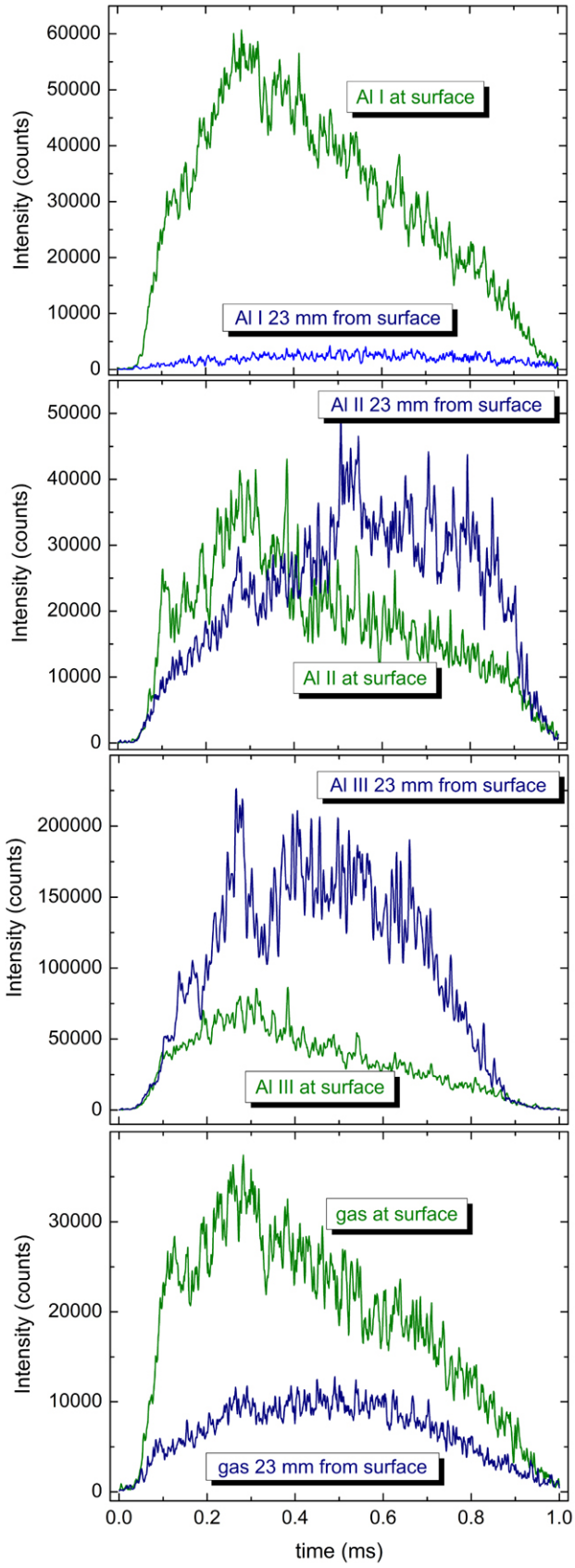
Al I at surface
Al I 23 mm from surface
Al II 23 mm from surface
Al II at surface
Al III 23 mm from surface
Al III at surface
gas at surface
gas 23 mm from surface
Intensity (counts)
time (ms)

Fig. 5

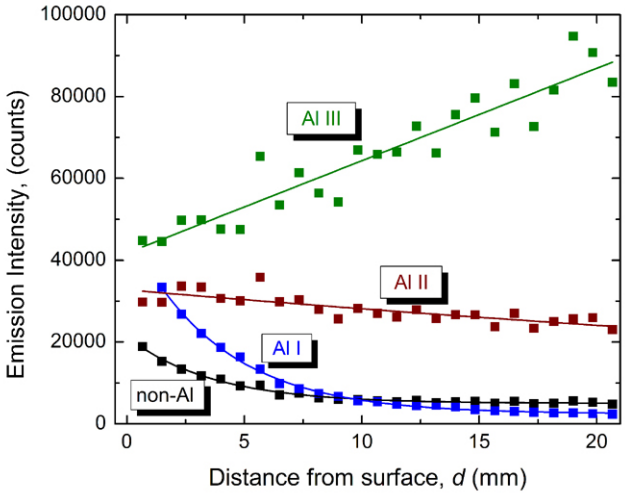
Emission Intensity, (counts)
Distance from surface, d (mm)
Al III
Al II
Al I
non-Al
0
20000
40000
60000
80000
100000
0
5
10
15
20

Fig. 6